



# Bioluminescent detection of zearalenone using recombinant peptidomimetic *Gaussia* luciferase fusion protein

Riikka Peltomaa<sup>1</sup> · Sabrina Fikacek<sup>1</sup> · Elena Benito-Peña<sup>1</sup>  · Rodrigo Barderas<sup>2</sup> · Trajen Head<sup>3,4</sup> · Sapna Deo<sup>3,4</sup> ·  
Sylvia Daunert<sup>3,4,5</sup> · María C. Moreno-Bondi<sup>1</sup>

Received: 23 May 2020 / Accepted: 28 August 2020 / Published online: 4 September 2020  
© Springer-Verlag GmbH Austria, part of Springer Nature 2020

## Abstract

The development of a bioluminescent immunosensor is reported for the determination of zearalenone (ZEA) based on a peptide mimetic identified by phage display. The peptide mimetic GW, with a peptide sequence GWWGPYGEIELL, was used to create recombinant fusion proteins with the bioluminescent *Gaussia* luciferase (GLuc) that were directly used as tracers for toxin detection in a competitive immunoassay without the need for secondary antibodies or further labeling. The bioluminescent sensor, based on protein G-coupled magnetic beads for antibody immobilization, enabled determination of ZEA with a detection limit of 4.2 ng mL<sup>-1</sup> (corresponding to 420 µg kg<sup>-1</sup> in food samples) and an IC<sub>50</sub> value of 11.0 ng mL<sup>-1</sup>. The sensor performance was evaluated in spiked maize and wheat samples, with recoveries ranging from 87 to 106% (RSD < 20%, n = 3). Finally, the developed method was applied to the analysis of a naturally contaminated reference matrix material and good agreement with the reported concentrations was obtained.

**Keywords** Bioluminescence · *Gaussia* luciferase · Mycotoxin · Zearalenone · Food safety

## Introduction

Mycotoxins, which are commonly encountered as food and feed contaminants, are secondary metabolites produced by

**Electronic supplementary material** The online version of this article (<https://doi.org/10.1007/s00604-020-04538-7>) contains supplementary material, which is available to authorized users.

- ✉ Elena Benito-Peña  
elenabp@ucm.es
- ✉ María C. Moreno-Bondi  
mcmbondi@ucm.es

<sup>1</sup> Department of Analytical Chemistry, Faculty of Chemistry, Complutense University, Ciudad Universitaria s/n, 28040 Madrid, Spain

<sup>2</sup> Chronic Disease Programme, UFIEC, Instituto de Salud Carlos III, Ctra. Majadahonda-Pozuelo Km 2.2, 28220 Madrid, Spain

<sup>3</sup> Department of Biochemistry and Molecular Biology, Miller School of Medicine, University of Miami, Miami, FL 33136, USA

<sup>4</sup> Dr. JT Macdonald Foundation Biomedical Nanotechnology Institute, University of Miami, Coral Gables, FL 33136, USA

<sup>5</sup> University of Miami Clinical and Translational Science Institute, University of Miami, Miami, FL 33136, USA

filamentous fungi. These toxins have a wide range of harmful effects of the neurotoxic, carcinogenic, and immunotoxic types on humans and other vertebrates; also, they alter their development and reproductive functions [1–3]. Aflatoxins, ochratoxins, fumonisins, trichothecenes, and zearalenone are among the major mycotoxins produced by ubiquitous fungal species [3, 4]. Zearalenone (ZEA) is a nonsteroidal estrogenic mycotoxin produced by various *Fusarium* species but particularly *F. graminearum*. By virtue of their similarity to 17β-estradiol, ZEA and some of its metabolites can bind competitively to estrogen receptors [1, 5]. ZEA occurs worldwide but especially in temperate and warm regions, where *Fusarium* species frequently colonize a number of cereal crops including wheat, maize, barley, oats, rice, and sorghum [6].

The detrimental toxic effects of mycotoxins and the economic burden of contamination with these fungi have led several international institutions, such as the European Commission [7, 8] and the US Food and Drug Administration [9], to establish maximum allowed levels for the major mycotoxins in food and feed with a view to protecting consumers' health. Current maximum limits for ZEA in Europe vary from 20 to 3000 µg kg<sup>-1</sup> depending on the foodstuffs or animal feed in question [7, 10]. A number of methods for mycotoxin analysis use liquid chromatography (LC) with diode array, fluorescence, or mass

spectrometric (MS) detection [11, 12]. For example, high-performance liquid chromatography (HPLC) coupled with fluorescence [13, 14] or MS detection [15, 16] have been described for ZEA detection. Although chromatographic analysis is very accurate and reproducible, its practical use is limited by its high cost and sluggishness. Biosensors and bioanalytical assays can overcome some of the shortcomings of chromatographic methods (particularly as regards cost and expeditiousness), so they can be useful supplements for sensitive and specific food safety analyses on the grounds of operational simplicity, throughput, and economy [17–19].

Several examples of assays based on antibodies [20–22] or aptamers [23, 24] as the biorecognition elements have proven their value as analytical tools for ZEA detection. Nevertheless, the development of immunosensors for mycotoxins and other low-molecular-weight contaminants is frequently hindered by the small size of the analyte, which often requires using a competitive assay format [25, 26]. The assays require conjugating the target molecule to a carrier protein or label for further immobilization or detection [27]. Preparing some analyte-conjugates can be a tough, time-consuming challenge or result in randomly cross-linked or unstable molecules that may severely restrict the sensitivity and accuracy of the assay. Peptide mimetics, also known as mimotopes, have been deemed a promising choice for overcoming the above-mentioned constraints thanks to their ability to bind to the same antibody paratope by mimicking the analyte's epitope [25, 26].

A number of low-molecular-weight targets, including pesticides [28], neurotoxins [29], cancer drugs [30], and mycotoxins [31–33], have been used as analytes in applications with peptide mimetics. Phage display can provide an elegant method for identifying peptide mimetics from phage-displayed peptide libraries even with no prior knowledge of the antibody's paratope [34–36]. Using phage-borne peptides provides a simple strategy for mycotoxin detection; however, the large size and biological activity of the phage virion limit their application for biosensing purposes [35, 37]. Synthetic peptide mimetics [38–41] and recombinant peptide–protein fusions [41–46] have been used as alternative, phage-free options. Specifically, recombinant fusions with either fluorescent [41, 42, 45] or bioluminescent proteins [46] have shown great potential as they allow the fusion protein to be directly used as a label without the need for secondary antibodies or further labeling. Moreover, the low cost of protein production in bacterial expression systems makes the use of recombinant fusion proteins particularly appealing. On the other hand, recombinant fusion proteins comprise of a fixed stoichiometry between the fusion partners, thus avoiding issues related to batch-to-batch variations often observed as the product of chemical conjugation reactions.

In this work, we developed a bioluminescence sensing platform for the analysis of ZEA based on a recombinant peptide mimetic tagged with a bioluminescent protein. ZEA peptide

mimetics were selected from a phage-displayed peptide library, and the newly identified ZEA-mimetic was used to construct a recombinant fusion protein with bioluminescent luciferase from *Gaussia* (GLuc; Fig. 1a–c). GLuc, which has been originally isolated from copepod *Gaussia princeps*, exhibits high luminescence emission and has proved a useful reporter protein for bioluminescent detection [47, 48]. The GLuc-tagged peptide mimetic was used to detect ZEA in a competitive immunoassay without the need of secondary antibodies (Fig. 2). The peptide mimetic competed for antibody binding with ZEA in the sample, and upon addition of the GLuc substrate, bright bioluminescence signals could be measured and correlated with the concentration of ZEA in the sample. The intrinsic nature of GLuc bioluminescence allowed measurements to be made without an excitation light source, which is a great advantage over fluorescent labels.

## Experimental

### Materials

Amylose resin and Ph.D.-12 Phage Display Peptide Library Kit, pMAL-c5X vector, and SHuffle Express Competent *Escherichia coli* were all obtained from New England Biolabs (Ipswich, MA, USA). The monoclonal anti-zearalenone antibody was from Soft Flow Hungary Ltd. (Pécs, Hungary), and the anti-fumonisins and anti-T-2 toxin antibodies were supplied by BioTez (Berlin, Germany). Clear and black MaxiSorp 96-well plates, black Packard HTRF 96-well plates, Dynabeads Protein G, Pierce Centrifuge Columns, Casein Blocker, and 1-Step Ultra TMB-ELISA were purchased from Thermo Fisher Scientific (Waltham, MA, USA). Bovine serum albumin (BSA) was from NZYTech (Lisbon, Portugal). The mycotoxins zearalenone (ZEA) and β-zearalenol were supplied by Sigma-Aldrich (St. Louis, MO, USA), whereas fumonisins B<sub>1</sub> and B<sub>2</sub>, deoxynivalenol, T-2 toxin, and ochratoxin A were from Fermentek Ltd. (Jerusalem, Israel).

Horseradish peroxidase (HRP)-conjugated anti-M13 antibody was purchased from GE Healthcare Inc. (Chicago, IL, USA) and KOD Xtreme Hot Start Master Mix from Millipore (Billerica, MA, USA). Protease Inhibitor Cocktail and D-(+)-maltose monohydrate were obtained from Sigma-Aldrich and native coelenterazine from NanoLight Technology (Pinetop, AZ, USA). The blank wheat quality control material was from Romer Labs (Getzersdorf, Austria) and the reference matrix material (zearalenone in corn) from Aokin AG (Berlin, Germany). Blank maize samples were obtained from an external laboratory specialized in mycotoxin analysis in Spain and analyzed with ultra-performance liquid chromatography coupled with mass spectrometry detectors (UPLC-MS/MS) to confirm that the samples were not contaminated with ZEA [15].

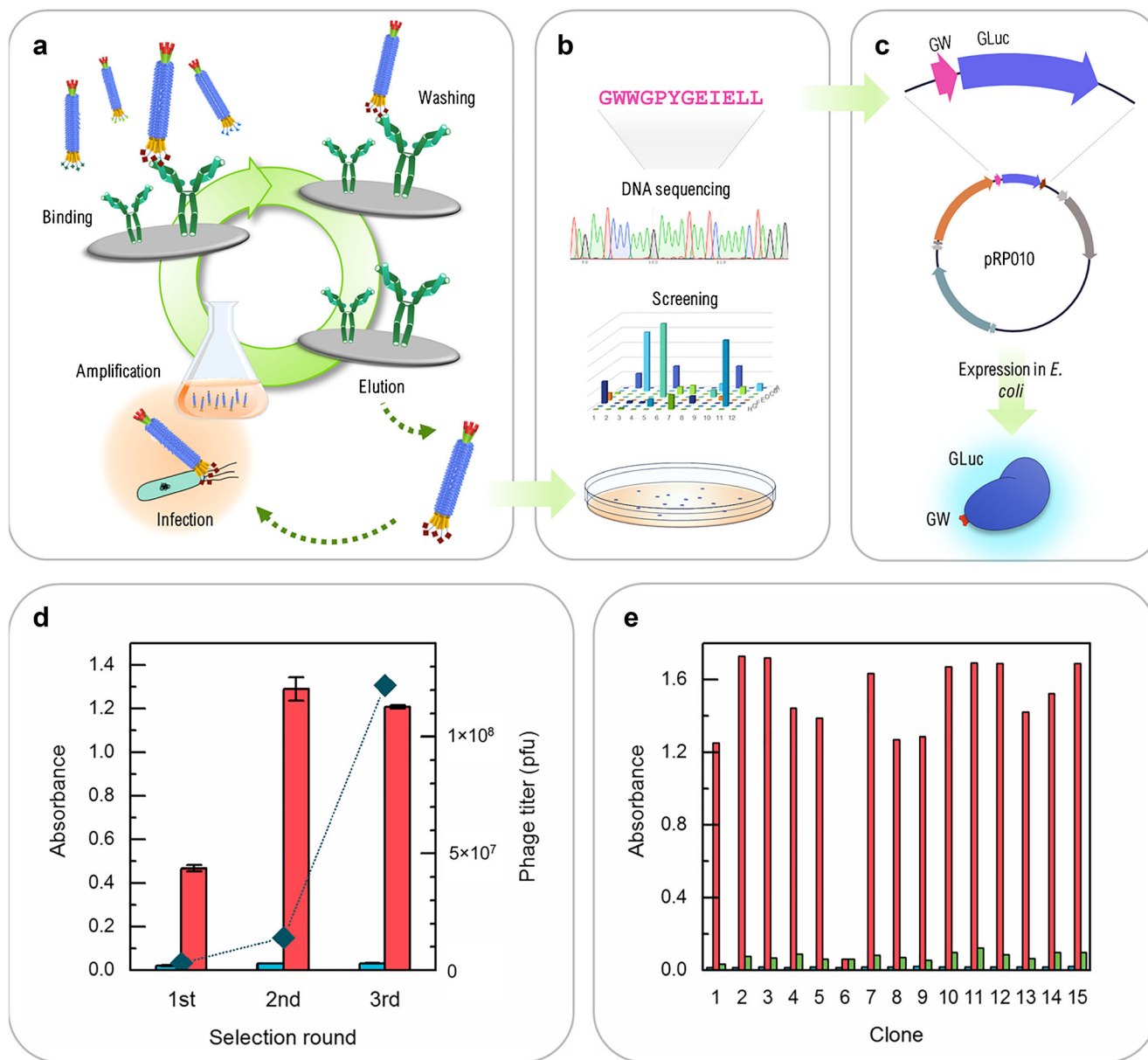


**Fig. 1** Workflow of the selection of zearalenone mimotopes by phage display and the subsequent construction of the fusion protein. **(a)** The selection process consisted of binding, washing, elution, and amplification steps, which were repeated three times to enrich the specific binders against anti-zearalenone antibody. **(b)** Target specificity of individual clones was determined by screening the monoclonal clones from single colonies in a phage-based ELISA, and the amino acid sequence of the positive clones was identified by DNA sequencing. **(c)** After identifying the sequence of the GW-peptide, it was used to construct a recombinant peptidomimetic fusion protein with *Gaussia luciferase* (GLuc). The fusion protein was expressed in *Escherichia coli* and used to develop the bioluminescent assay for the detection of zearalenone (see also Fig. 2). **(d)** After the selection rounds, the polyclonal phage-based ELISA showed specific binding to the target antibody (red) and low nonspecific binding to background wells (blue) coated with BSA ( $n = 2$ ). Likewise, enrichment of the phages was observed in the phage titers after each selection round (blue diamonds; right y-axis). **(e)** Monoclonal phage-based ELISA with 15 individual clones (1:30 dilution) showed high specific binding to the target antibody (red) with all except one clone, and low signals were measured in the background wells (blue) and in the presence of free zearalenone ( $1 \mu\text{g mL}^{-1}$ ; green), demonstrating the competition between the mimotope and the toxin. Scheme of the phage-based assay is shown in Fig. S1a

also Fig. 2). (d) After the selection rounds, the polyclonal phage-based ELISA showed specific binding to the target antibody (red) and low nonspecific binding to background wells (blue) coated with BSA ( $n = 2$ ). Likewise, enrichment of the phages was observed in the phage titers after each selection round (blue diamonds; right y-axis). (e) Monoclonal phage-based ELISA with 15 individual clones (1:30 dilution) showed high specific binding to the target antibody (red) with all except one clone, and low signals were measured in the background wells (blue) and in the presence of free zearalenone ( $1 \mu\text{g mL}^{-1}$ ; green), demonstrating the competition between the mimotope and the toxin. Scheme of the phage-based assay is shown in Fig. S1a

## Selection of mimotopes by phage display

ZEA peptide mimetics were selected in consecutive rounds from a commercial dodecapeptide library (Ph.D.-12), using monoclonal anti-ZEA antibody as target and following the

manufacturer's instructions with minor modifications. In each round, wells of a 96-well microtiter plate were coated with anti-ZEA by overnight incubation at  $+4^\circ\text{C}$ . In the first round, three wells of a MaxiSorp plate were coated with  $1 \mu\text{g}$  of antibody in  $100 \mu\text{L}$  of  $0.1 \text{ mol L}^{-1}$  sodium bicarbonate buffer

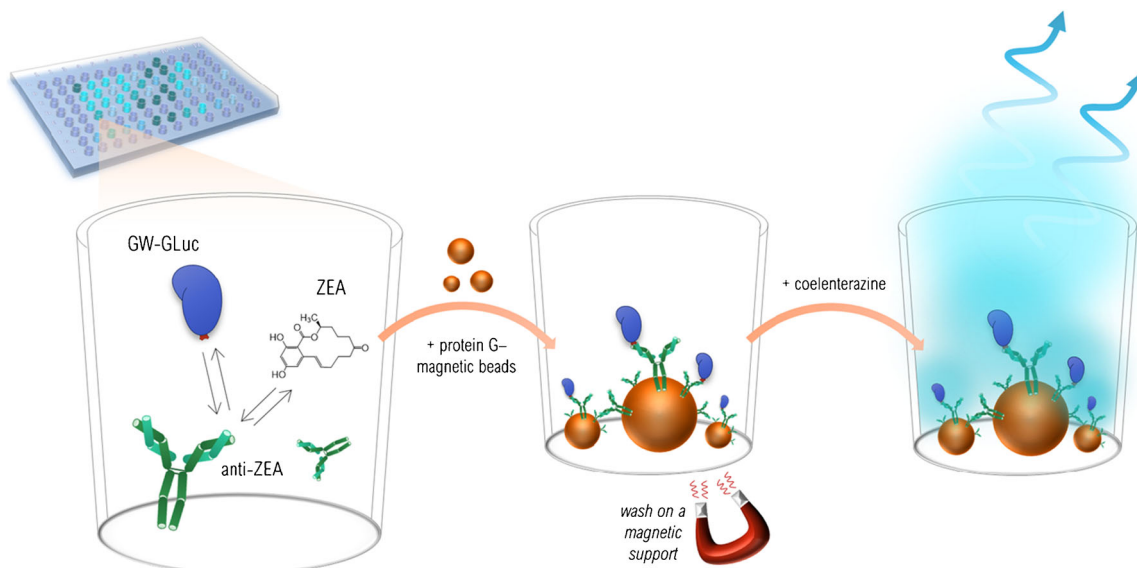


**Fig. 2** Detection of zearalenone (ZEA) based on the bioluminescent *Gaussia* luciferase (GLuc)-tagged peptide mimetic (GW). The amount of ZEA in the sample was determined through the competitive binding between ZEA and GW-GLuc to the anti-ZEA antibody, after which the

immunocomplex was captured using protein G-coupled magnetic beads and washed using a magnetic support. Finally, the bioluminescent signals were measured upon addition of coelenterazine, the GLuc substrate

per well; in subsequent rounds, however, the amount of antibody was reduced to 0.5  $\mu$ g and 0.25  $\mu$ g per well—and the number of wells to 2 in the second round and 1 in the third. Similarly, the wells for negative selection were coated with 100  $\mu$ L of 5 mg mL<sup>-1</sup> BSA. The day after coating, the wells were blocked with 3% (w/v) BSA in PBS (pH 7.2) at room temperature with slow shaking for 2 h. Then, they were rinsed three times with PBS-T [PBS (pH 7.2); 0.1% (v/v) Tween-20]. In the first selection round, 100-fold representation of the library (viz.,  $2 \times 10^{11}$  pfu for a library with  $2 \times 10^9$  clones) diluted in PBS with 0.05% (v/v) Tween-20 and 0.1% (w/v) BSA was added to BSA-coated wells without the target in order to remove unwanted binders against the background. The plates were then incubated at room temperature with slow shaking for 1.5 h. The solution was transferred to the wells coated with the target antibody, and incubation was continued for another 1.5 h. Then, the wells were rinsed six times with PBS-T, and bound phages were eluted with 100  $\mu$ L of 0.2 mol L<sup>-1</sup> glycine-HCl (pH 2.2) containing 0.01% (w/v) BSA for 10 min, the supernatant being immediately neutralized with 40  $\mu$ L of 1 mol L<sup>-1</sup> Tris-HCl (pH 9.1). The eluate was amplified by using it to infect *E. coli* ER2738 and purified by PEG precipitation according to the manufacturer's instructions [49]. The amplified phage was then used in the subsequent panning rounds. After each round, the number of eluted and amplified phages was determined by titering, and the number of input phages ( $2 \times 10^{11}$  pfu) was kept constant in all rounds. The incubation time in the preselection and target wells was shortened to 1 h in the second and third rounds, whereas the number of rinses was increased to 10 and the concentration of Tween-20 in the rinsing buffer from 0.1 to

0.5% (v/v) for more stringent rinsing. Elution of good ZEA mimetics was facilitated by using a competitive elution step instead of glycine. After rinsing, 100 ng mL<sup>-1</sup> ZEA in the second round and 10 ng mL<sup>-1</sup> ZEA in the third round was added to each well and incubated for 1 h, after which the solution was collected and used to infect the bacteria. After the three selection rounds, individual plaques were picked from the LB/IPTG/X-gal plates and subjected to phage-based enzyme-linked immunosorbent assay (ELISA) in order to select positive clones binding to the target antibody. Finally, peptide sequences were identified by sequencing the selected clones with the primer -96 gIII (5'-CCC TCA TAG TTA GCG TAA CG-3').

### Phage-based ELISA

Panning success was assessed by phage-based ELISA with immobilized anti-ZEA antibody and HRP-labeled anti-M13 secondary antibody (Fig. S1a). For this purpose, microtiter well plates were coated with anti-ZEA capture antibody (200 ng in 60  $\mu$ L of 0.2 mol L<sup>-1</sup> sodium carbonate/bicarbonate buffer, pH 9.4) by overnight incubation at + 4 °C. Specificity in the binding was confirmed using anti-fumonisins and anti-T-2 antibodies as controls. The wells were then blocked with blocking buffer [PBS, pH 7.2; 3% (w/v) BSA] for 2 h at +4 °C and rinsed twice with PBS-T [PBS, pH 7.2; 0.1% (v/v) Tween-20]. Next, the amplified phage stock was added to the coated wells in a 1:30 or 1:100 dilution and incubated for 1 h. For the competitive assay, the wells were additionally supplied with variable concentrations of ZEA (0–100 ng mL<sup>-1</sup>) or 100 ng mL<sup>-1</sup> of fumonisins B<sub>1</sub>, T-2

toxin, or deoxynivalenol. After rinsing each plate four times, anti-M13-HRP (1:5000 dilution in blocking buffer) was added and incubation allowed to continue for 1 h. All incubation steps were done in a total volume of 60  $\mu$ L under slow shaking at room temperature. Finally, plates were rinsed four times, and a 60  $\mu$ L volume of TMB substrate solution was added to each well. After 1–5-min incubation, the reaction was stopped by adding 60  $\mu$ L of 2 mol L<sup>-1</sup> sulfuric acid to each, and the absorbance was measured at 450 nm with a CLARIOstar microplate reader from BMG Labtech (Ortenberg, Germany).

### Construction of the bioluminescent fusion protein

For expression of GLuc-tagged peptide mimetic, the *GLuc* gene was PCR-amplified from vector pColdI-GLuc [50] using KOD Xtreme Hot Start Master Mix. The DNA sequence encoding for the peptide mimetic GW (GWWGPYGEIELL) and the GS-linker were added to the 5'-end, and so was a polyhistidine tag to the 3'-end of *GLuc* in three sequential PCR-reactions involving the primers listed in Table S1 in the supporting information (1st PCR: Forward Primer 1 and Reverse Primer 1; 2nd PCR: Forward Primer 2 and Reverse Primer 2; 3rd PCR: Forward Primer 3 and Reverse Primer 2). The product from the third PCR-reaction was then subcloned to a pMAL-c5X expression vector at NdeI and BamHI sites.

### Fusion protein expression and purification

For overexpression of the GLuc-tagged peptide mimetic (GW-GLuc), the plasmid encoding for the fusion protein (Fig. S2a) was transformed into *E. coli* SHuffle Express cells and selected on LB agar plates with 100  $\mu$ g mL<sup>-1</sup> ampicillin. A single colony harboring the plasmid was used to inoculate a 5-mL preculture (LB medium supplemented with 100  $\mu$ g mL<sup>-1</sup> ampicillin) that was grown at +37 °C under stirring at 250 rpm overnight. The following day, the overnight preculture was expanded into the main culture of 180 mL (LB medium supplemented with 100  $\mu$ g mL<sup>-1</sup> ampicillin), and growth was continued at +37 °C until an optical density at 600 nm (OD<sub>600</sub>) of 0.7 was reached. Protein expression was then induced with isopropyl  $\beta$ -D-1-thiogalactopyranoside (IPTG) at a final concentration of 1 mmol L<sup>-1</sup>, followed by growth at +15 °C for 4 h. The cells were collected by centrifugation (10 min at 5000 g at +4 °C) and resuspended in 10 mL of lysis buffer (50 mmol L<sup>-1</sup> Tris-HCl, pH 8.7; 150 mmol L<sup>-1</sup> NaCl) supplemented with the protease inhibitor cocktail. Cells were lysed by sonication on ice for 10 min, using 10 s on/off pulse cycles, after which the resulting cell debris was removed by centrifugation at +4 °C at 12000 g for 20 min, and the supernatant was passed through a 0.45- $\mu$ m syringe filter.

The clarified lysate was then incubated with 1 mL of amylose resin for 30 min, collected on a Pierce

Centrifuge Column by gravity flow, and washed with 10 column volumes of lysis buffer. Next, the protein was eluted in 1 mL fractions with lysis buffer supplemented with 10 mmol L<sup>-1</sup> maltose. Purification was followed by SDS-PAGE analysis (Fig. S2b), and the protein concentration of the purified stock was determined spectrophotometrically. The bioluminescence emission spectra (Fig. S1c) of the purified protein was measured with CLARIOstar immediately after injecting 60  $\mu$ L of native coelenterazine (2.0  $\mu$ g mL<sup>-1</sup> in PBS) to the well.

### Bioluminescence-based detection of zearalenone

The detection of ZEA with GLuc-tagged peptide mimetic (GW-GLuc) was performed in a microtiter well plate by immobilizing the capture antibody on the plate by absorption (plate-based assay) or using magnetic beads modified with protein G to capture the antibody (bead-based assay).

In the plate-based method, the wells of a black MaxiSorp plate were coated with anti-ZEA antibody (50 ng in 60  $\mu$ L of 0.2 mol L<sup>-1</sup> sodium carbonate/bicarbonate buffer, pH 9.4) by overnight incubation at +4 °C. The wells were then blocked with blocking buffer [PBS, pH 7.2; 3% (w/v) BSA] at room temperature for 4 h and rinsed twice with PBS-T [PBS, pH 7.2; 0.05% (v/v) Tween-20]. Toxin standards ranging from 0 to 100 ng mL<sup>-1</sup> in concentration were added in triplicate to the coated wells together with 48 ng of GW-GLuc in assay buffer [PBS, pH 7.2; 0.05% (v/v) Tween-20; 0.1% (w/v) BSA] in a total reaction volume of 60  $\mu$ L. After incubation under slow shaking for 1.5 h, the wells were washed with PBS-T four times. Finally, the total bioluminescence intensity of each well was measured with the CLARIOstar after injecting 60  $\mu$ L of native coelenterazine at a final concentration of 2.0  $\mu$ g mL<sup>-1</sup> in PBS.

In the bead-based method, the wells of a black HTRF plate were first blocked with Casein blocker at +37 °C for 1 h. Then, they were rinsed twice, and 48 ng of GW-GLuc was mixed with 100 ng of anti-ZEA antibody together with toxin standards spanning the concentration range 0–100 ng mL<sup>-1</sup> in triplicate in a total reaction volume of 60  $\mu$ L, using the same assay buffer as in the plate-based assay. After incubation with shaking at room temperature for 1 h, protein G beads (10  $\mu$ g in 40  $\mu$ L) were added to each well, and incubation was allowed to continue for another 30 min. Then, beads were rinsed three times with PBS-T in a plate washer furnished with a magnetic support (HydroFlex, Tecan, Switzerland). Finally, the bioluminescence intensity was measured as described above.

### Spiking

Blank maize or wheat samples (1 g) were spiked by adding a known amount of mycotoxin stock solution (spiking

levels from 700 to 1250  $\mu\text{g kg}^{-1}$ ). Then, they were kept at +35 °C for 3 days to facilitate evaporation of the solvent from the stock solution (1 mg mL<sup>-1</sup> stock of ZEA in acetonitrile) and also to allow the analyte and matrix to equilibrate.

### Sample extraction

The mycotoxin was extracted from the blank, the spiked samples, or the reference material by following a preset protocol that was previously found to provide the optimum compromise in the extraction of mycotoxins from wheat and maize [51]. Briefly, 5 mL of extractant (viz., 79:20:1 v/v acetonitrile/water/acetic acid) was added to 1 g of maize or wheat sample, and the sample was extracted under shaking at 120 rpm at room temperature for 60 min and then centrifuged at 15000 g for 15 min. The resulting extract was passed through a 0.22-μm filter and diluted in assay buffer before analysis with the bead-based immunoassay. For the spiked samples, 5% (v/v) extract was used in the final reaction volume for the assay to avoid interference of the matrix.

### Data analysis

The total bioluminescence signals obtained with different toxin concentrations were normalized to the minimum and maximum levels, which were then analyzed with the software Origin Pro 9.0 (OriginLab Corp., Northampton, MA, USA), using a four-parameter logistic regression (4-PL) model:

$$y = A_{\min} + \frac{(A_{\max} - A_{\min})}{1 + \left(\frac{x}{IC_{50}}\right)^b} \quad (1)$$

where  $A_{\max}$  is the asymptotic maximum (viz., the signal in the absence of analyte),  $A_{\min}$  is the asymptotic minimum, and  $b$  and  $IC_{50}$  are the slope of the curve and the analyte concentration at the inflection point, respectively. The limit of detection (LOD) was determined as the toxin concentration where antibody binding to the peptide was inhibited by 10% and the dynamic range as the toxin concentration corresponding to 20–80% inhibition as described elsewhere [52]. Cross-reactivity (CR) was calculated from  $IC_{50}$  values, using the following equation:

$$CR = \frac{IC_{50}(\text{ZEA})}{IC_{50}(\text{other mycotoxins})} \times 100\% \quad (2)$$

The apparent recovery from each spiked sample was calculated as the ratio of observed toxin concentration to the reference value.

## Results and discussion

### Selection and characterization of phage-displayed zearalenone peptide mimetics

Zearalenone (ZEA) peptide mimetics were selected from the linear 12-mer phage display peptide library (Ph.D.-12) in three successive rounds of panning (Fig. 1a). The first round was performed with a high concentration of the target antibody and gentle washes to maximize the capture of all interesting clones, whereas during the subsequent rounds, the amount of the antibody was reduced, and the stringency of the washes was increased. Moreover, the elution step in the second and third rounds was performed by competition with decreasing amounts of free toxin instead of the nonspecific acid elution used in the first round. The use of these strategies for the selections allowed an efficient enrichment of antibody binding phages during the three selection rounds. This observation was evidenced by an increase in the phage titers during the panning rounds and by the excellent signal-to-background ratios observed in the ELISA using the entire phage pools after each panning round (Fig. 1d). A total of 15 individual phage clones were randomly selected from the third panning round, amplified, and tested similarly in the phage-based ELISA. Altogether, 14 out of 15 clones tested showed good signal-to-background ratios in the assays indicating specific binding to the anti-ZEA antibody. Moreover, competition with the free ZEA (1000 ng mL<sup>-1</sup>) was seen with all the 14 clones demonstrating a successful selection of peptide mimetics (Fig. 1e).

The DNA sequencing (Fig. 1b) results showed two conserved peptide sequences, GWWGPYGEIELL and SFDYFLWDSTET (named GW and SF, respectively), which were further tested in the competitive ELISAs with different toxin concentrations (Fig. S1b). Clone GW showed a better response in terms of sensitivity and reproducibility and was selected for further applications. Cross-reactivity studies with other mycotoxins, or other mycotoxin-specific antibodies, demonstrated the GW-peptide to be specific for the target anti-ZEA antibody and an excellent mimetic of ZEA (Fig. S1c–d).

### Bioluminescent detection based on GLuc fusion protein

The bioluminescent immunosensor for ZEA detection (Fig. 2) was established for a simple analysis of the mycotoxin in cereals. Recombinant peptidomimetic fusions were constructed based on bioluminescent GLuc in fusion with the newly identified peptide mimetic GW (Fig. 1c and S2a). The GLuc-tagged peptide (GW-GLuc) could be produced cost-effectively in bacteria readily linked to a bioluminescent protein label which functioned as the tracer for the toxin

detection. The fusion protein exhibited bright bioluminescence upon addition of the GLuc substrate, and thus, neither secondary antibodies nor separate labeling reactions with additional purification steps were required for the assay development (Fig. S2b–c).

The epitope-mimicking nature of the recombinant fusion proteins and their functionality as the tracer was confirmed by immobilizing the capture antibody in microtiter wells and observing the competitive binding between ZEA and the GW-GLuc as low luminescence readings in the presence of high toxin concentrations. Based on a sigmoidal standard curve (Fig. S3), the half-maximal inhibitory concentration ( $IC_{50}$ ) and the limit of detection (LOD) were  $15.6 \text{ ng mL}^{-1}$  and  $7.9 \text{ ng mL}^{-1}$ , respectively. In order to improve the sensitivity and broaden the dynamic range ( $10.4\text{--}23.6 \text{ ng mL}^{-1}$ ) of the plate-based biosensor, the method was adapted to a bead-based format. The competition step was carried out in solution and protein G-coupled magnetic beads were added afterwards for capturing and washing the immunocomplex. In agreement with previous reports [41], the bead-based method improved the sensitivity as well as slightly the dynamic range in comparison with the plate-based method (Fig. S3). The  $IC_{50}$  value and the LOD of the bead-based immunosensor were  $11.0 \text{ ng mL}^{-1}$  and  $4.2 \text{ ng mL}^{-1}$ , respectively. The dynamic range (20–80% inhibition) was between  $6.2$  and  $19.6 \text{ ng mL}^{-1}$ . The intraday ( $n=3$ ) relative standard deviation (RSD) was 8.2% on average, while the interday value for assays performed on three different days was 10.6%. Moreover, the stability of GW-GLuc was evaluated, and the peptidomimetic fusion protein was observed to be stable during at least 8 weeks when stored at  $+4^\circ\text{C}$  or  $-20^\circ\text{C}$ .

The sensitivity of the developed bioluminescent immunosensor is comparable or better than the sensitivity of commercially available ELISA kits (e.g.,  $5 \text{ ng mL}^{-1}$  for the Zearalenone ELISA supplied by Demeditec Diagnostics GmbH (Germany) [53],  $6 \text{ ng mL}^{-1}$  for the Zearalenone ELISA kit of BioVision (USA) [54], or  $20 \text{ ng mL}^{-1}$  AgraQuant Zearalenone Plus from Romer Labs (Austria)) [55]. Although other immunoassays based on peptide mimetics for ZEA detection have very recently reported significantly lower detection limits (down to  $\text{fg mL}^{-1}$ ) [56, 57], the bioluminescent biosensor benefits from a straightforward measurement scheme as well as a lower cost, as no labeled secondary antibodies are required (Table S2). Moreover, since the peptide mimetic is produced directly tagged with the GLuc, it does not require any further modification or labeling. On the other hand, also the simplicity of the bioluminescent measurement is an advantage as no external excitation light is required and can be easily implemented in commercial devices.

### Cross-reactivity

The specificity of the method was determined by analyzing other mycotoxins produced by the same *Fusarium* species as

ZEA. No significant cross-reactivity was observed with fumonisins B<sub>1</sub> or B<sub>2</sub>, deoxynivalenol, nor ochratoxin A. Nonetheless,  $\beta$ -zearalenol which is one of the major metabolites of ZEA showed a similar response as ZEA with an  $IC_{50}$  value of  $13.6 \text{ ng mL}^{-1}$  leading to cross-reactivity of 81% (Fig. 3). The specific cross-reactivity for the anti-ZEA antibody used in this work is not available by the supplier; however, as reported in the literature, anti-ZEA antibodies usually show cross-reactivity with the main mycotoxin analogues; therefore, they can be applied for the screening of the mycotoxin and related metabolites [58]. In any case, according to the European Food Safety Authority (EFSA), there is limited evidence of the presence of  $\beta$ -zearalenol in food [5]; therefore, it should not be a problem for the analysis.

### Matrix effect

The effect of the sample matrix for the assay response was studied by completing the toxin calibration in the presence of the sample extract. Blank maize and wheat samples were

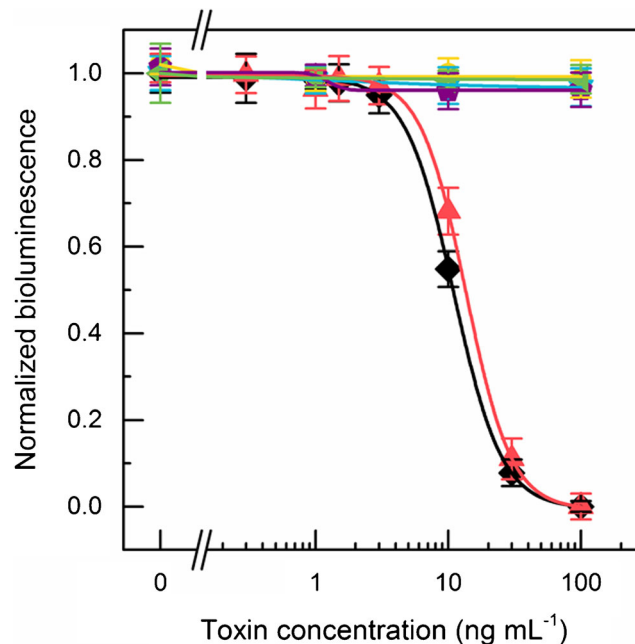


**Fig. 3** Bead-based bioluminescent immunosensor with different mycotoxins, i.e., ZEA (black diamonds),  $\beta$ -zearalenol (red triangles), fumonisins B<sub>1</sub> (yellow circles) and B<sub>2</sub> (blue triangles), deoxynivalenol (purple pentagons), and ochratoxin A (green down triangles). Toxins ranging from 0 to  $100 \text{ ng mL}^{-1}$  were mixed with  $48 \text{ ng}$  of the GW-GLuc diluted in the assay buffer (PBS, pH 7.2; 0.05% (v/v) Tween-20; 0.1% (w/v) BSA). The total bioluminescence intensity of each well was measured with the CLARIOstar after injecting  $60 \mu\text{L}$  of native coelenterazine ( $2.0 \mu\text{g mL}^{-1}$  in PBS). The bioluminescence values were normalized to the mean maximum and minimum signals, and the results are shown as normalized means  $\pm$  the standard error of the mean ( $n=3$ ). Four-parametric logistic fit (OriginPro 2019) was used to calculate the  $IC_{50}$  values

treated according to a previously reported mycotoxin extraction protocol [51], and different percentages of the sample extract were included in the analysis. In comparison with the response in assay buffer, high percentages of the sample extract (10–15%) showed inferior performance, but no significant matrix effects were observed with 5% maize or wheat extracts (Fig. 4) that were selected for the subsequent experiments.

## Sample analysis

Blank maize and wheat samples were spiked with the toxin standard in different concentrations, in the range of 700–1250  $\mu\text{g kg}^{-1}$ , and measured using the bead-based bioluminescent biosensor. Taking into account the sample extraction protocol and the dilution factor, these correspond to final concentrations of 7–12.5  $\text{ng mL}^{-1}$  in the assay. Mean recoveries of 91–106% in maize and 87–97% in wheat were observed (Table 1). Finally, the accuracy of the method was evaluated by analyzing a naturally contaminated reference matrix material. The results (Table 2) were in good accordance with the reported contamination level with no statistically significant differences (95% confidence level) demonstrating the applicability of the method to the analysis of naturally contaminated cereal samples. Future work aims to optimize the sample extraction protocol to increase the sensitivity of the method.

**Table 1** Analysis of spiked wheat and maize samples

Matrix	Spiked ( $\mu\text{g kg}^{-1}$ )	Measured ( $\mu\text{g kg}^{-1}$ )	RSD	Recovery
Maize	700	667	14%	95%
	800	800	9%	106%
	1000	944	6%	94%
	1250	1153	4%	92%
Wheat	700	610	19%	87%
	800	759	15%	95%
	1000	966	7%	97%
	1250	1157	7%	93%

## Conclusions

In this work, we used phage display technology to select a zearalenone mimicking peptides from a commercial peptide library. Also, we developed a bioluminescent biosensor using recombinant peptidomimetic GLuc-fusion proteins based on the zearalenone the mimetic GW. The bioluminescence-based method proved simpler than the phage-based assay because it allowed the GLuc-tagged peptide to be used directly as the tracer. The bioluminescent bead-based biosensor, which exhibited good analytical performance, was used to analyze spiked and naturally contaminated cereal samples with promising results. No significant cross-reactivity was observed with other mycotoxins produced by the same fungi species; however,  $\beta$ -

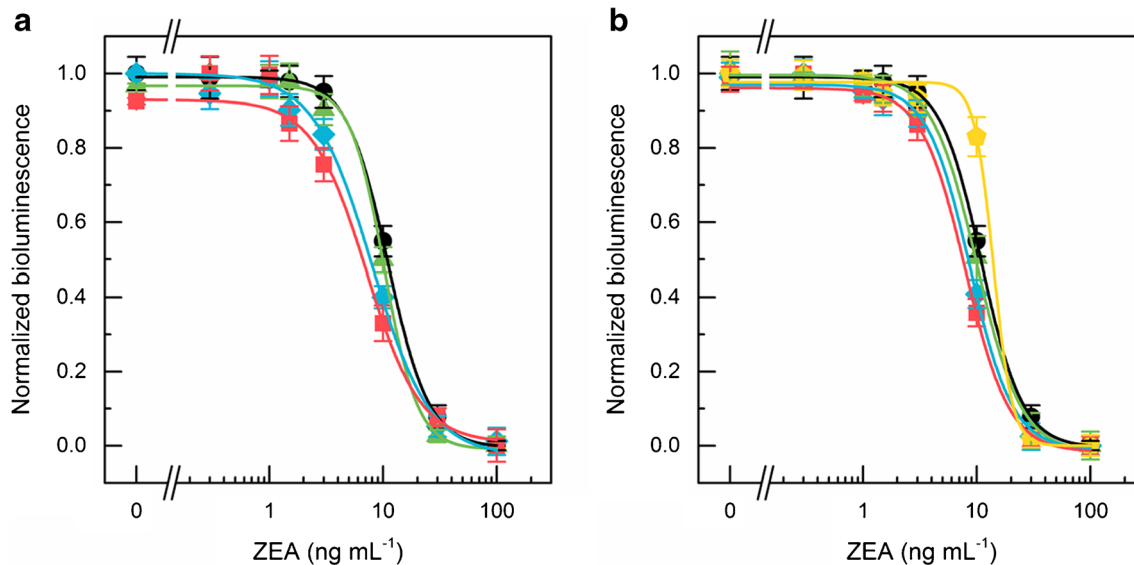


**Fig. 4** Comparison of the calibration curves in the assay buffer (black circles) or in the presence of 5% (green triangles), 7% (blue diamonds), 10% (red squares), or 15% (yellow pentagons) of the sample extracts. The effect of (a) maize and (b) wheat samples was compared. ZEA ranging from 0 to 100  $\text{ng mL}^{-1}$  was mixed with 48 ng of the GW-GLuc diluted in the assay buffer (PBS, pH 7.2; 0.05% (v/v) Tween-20; 0.1% (w/v) BSA) supplemented with different concentrations of the blank sample extract.

The total bioluminescence intensity of each well was measured with the CLARIOstar after injecting 60  $\mu\text{L}$  of native coelenterazine (2.0  $\mu\text{g mL}^{-1}$  in PBS). The luminescence values were normalized to the mean maximum and minimum signals, and the results are shown as normalized means  $\pm$  the standard error of the mean ( $n = 3$ ) and fitted to a four-parametric logistic fit (OriginPro 2019)

**Table 2** Analysis of the reference materials

Sample	Reported ( $\mu\text{g kg}^{-1}$ )	Measured ( $\mu\text{g kg}^{-1}$ )*
Maize	884 $\pm$ 265	787 $\pm$ 123
	1688 $\pm$ 506	1361 $\pm$ 222

\* $\text{ts}/\sqrt{n}$ ,  $t_{95\%}$ ,  $n = 3$

zearalenol, one of the major metabolites of ZEA, shows appreciable cross-reactivity; therefore, in principle, the assay could be applied for the screening of the mycotoxin and its related metabolite. In future work, the method could be integrated into a simple platform to take advantage of the simplicity of the assay format and bioluminescent measurements.

**Acknowledgments** Belén Patiño from the Department of Biology (Universidad Complutense de Madrid) is gratefully acknowledged for providing the blank maize samples analyzed in this work.

**Authors' contributions** The manuscript was written through contributions of all authors, and all authors have given approval to the final version of the manuscript.

**Funding** This study was supported by the Spanish Ministry of Science, Innovation and Universities (RTI2018-096410-B-C21). R.P. acknowledges UCM for a research grant. S. Daunert and S. Deo would like to thank the National Institutes of Health, NIGMS (R01GM114321, R01GM127706). This work was also supported by the National Science Foundation grant (CHE-1506740, CBET-1841419) to S. Daunert and S. Deo. S. Daunert is grateful to the Miller School of Medicine of the University of Miami for the Lucille P. Markey Chair in Biochemistry and Molecular Biology.

### Compliance with ethical standards

**Conflict of interest** The authors declare that they have no conflict of interest.

### References

1. Bennett JW, Klich M (2003) Mycotoxins. *Clin Microbiol Rev* 16: 497–516. <https://doi.org/10.1128/CMR.16.3.497-516.2003>
2. DeVries JW, Trucksess MW, Jackson LS (2002) Mycotoxins and food safety. Springer, New York, NY, USA
3. Council for Agricultural Science and Technology, CAST (2003) Mycotoxins: risks in plant, animal, and human systems. Council for agricultural science and technology. Ames, Iowa
4. Bräse S, Encinas A, Keck J, Nising CF (2009) Chemistry and biology of mycotoxins and related fungal metabolites. *Chem Rev* 109:3903–3990. <https://doi.org/10.1021/cr050001f>
5. European Food Safety Authority, EFSA Panel on Contaminants in the Food Chain (2017) Risks for animal health related to the presence of zearalenone and its modified forms in feed. *EFSA J* 15: 2197. <https://doi.org/10.2903/j.efsa.2017.4851>
6. Goyal S, Ramawat KG, Mérillon JM (2016) Different shades of fungal metabolites: an overview. In: Mérillon J-M, Ramawat KG (eds) *Fungal Metabolites*. Springer, Cham
7. European Commission (2006) Commission regulation (EC) no 1881/2006. *Off J Eur Union* L364:5–24
8. European Commission (2007) Commission regulation (EC) no 1126/2007. *Off J Eur Union* L255:14–17
9. U.S. Food and Drug Administration (FDA). [www.fda.gov/food/guidanceregulation/](http://www.fda.gov/food/guidanceregulation/). Accessed 28 July 2020
10. European Commission (2006) Commission recommendation (EC) no 576/2006. *Off J Eur Union* L229:7–10
11. De Saeger S (2011) Determining mycotoxins and mycotoxicogenic fungi in food and feed. Woodhead Publishing, Cambridge
12. Turner NW, Subrahmanyam S, Piletsky SA (2009) Analytical methods for determination of mycotoxins: a review. *Anal Chim Acta* 632:168–180. <https://doi.org/10.1016/j.aca.2008.11.010>
13. De Saeger S, Sibanda L, Van Peteghem C (2003) Analysis of zearalenone and  $\alpha$ -zearalenol in animal feed using high-performance liquid chromatography. *Anal Chim Acta* 487:137–143. [https://doi.org/10.1016/S0003-2670\(03\)00555-5](https://doi.org/10.1016/S0003-2670(03)00555-5)
14. Drzymala SS, Weiz S, Heinze J, Marten S, Prinz C, Zimathies A, Garbe LA, Koch M (2015) Automated solid-phase extraction coupled online with HPLC-FLD for the quantification of zearalenone in edible oil. *Anal Bioanal Chem* 407:3489–3497. <https://doi.org/10.1007/s00216-015-8541-5>
15. Romera D, Mateo EM, Mateo-Castro R, Gómez JV, Gimeno-Adelantado JV, Jiménez M (2018) Determination of multiple mycotoxins in feedstuffs by combined use of UPLC-MS/MS and UPLC-QTOF-MS. *Food Chem* 267:140–148. <https://doi.org/10.1016/j.foodchem.2017.11.040>
16. Hidalgo-Ruiz JL, Romero-González R, Martínez Vidal JL, Garrido Frenich A (2019) A rapid method for the determination of mycotoxins in edible vegetable oils by ultra-high performance liquid chromatography-tandem mass spectrometry. *Food Chem* 288:22–28. <https://doi.org/10.1016/j.foodchem.2019.03.003>
17. Köppen R, Koch M, Siegel D, Merkel S, Maul R, Nehls I (2010) Determination of mycotoxins in foods: current state of analytical methods and limitations. *Appl Microbiol Biotechnol* 86:1595–1612. <https://doi.org/10.1007/s00253-010-2535-1>
18. Berthiller F, Brera C, Crews C, Iha MH, Krska R, Lattanzio VMT, MacDonald S, Malone RJ, Maragos C, Solfrizzo M, Stroka J, Whitaker TB (2016) Developments in mycotoxin analysis: an update for 2014–2015. *World Mycotoxin J* 9:5–30. <https://doi.org/10.3920/WMJ2015.1998>
19. Turner NW, Bramhmbhatt H, Szabo-Vezse M, Poma A, Coker R, Piletsky SA (2015) Analytical methods for determination of mycotoxins: an update (2009–2014). *Anal Chim Acta* 901:12–33. <https://doi.org/10.1016/j.aca.2015.10.013>
20. Hervás M, López MA, Escarpa A (2011) Integrated electrokinetic magnetic bead-based electrochemical immunoassay on microfluidic chips for reliable control of permitted levels of zearalenone in infant foods. *Analyst* 136:2131–2138. <https://doi.org/10.1039/C1AN15081B>
21. Xu S, Zhang G, Fang B, Xiong Q, Duan H, Lai W (2019) Lateral flow immunoassay based on polydopamine-coated gold nanoparticles for the sensitive detection of zearalenone in maize. *ACS Appl Mater Interfaces* 11:31283–31290. <https://doi.org/10.1021/acsami.9b08789>
22. Yang M, Cui M, Wang W, Yang Y, Chang J, Hao J, Wang H (2020) Background-free upconversion-encoded microspheres for mycotoxin detection based on a rapid visualization method. *Anal Bioanal Chem* 412:81–91. <https://doi.org/10.1007/s00216-019-02206-1>
23. Azri FA, Eissa S, Zourob M, Chinnappan R, Sukor R, Yusof NA, Raston NHA, Alhoshani A, Jinap S (2020) Electrochemical determination of zearalenone using a label-free competitive aptasensor. *Microchim Acta* 187:266. <https://doi.org/10.1007/s00604-020-4218-7>

24. Xing K-Y, Peng J, Shan S, Liu DF, Huang YN, Lai WH (2020) Green enzyme-linked immunosorbent assay based on the single-stranded binding protein-assisted aptamer for the detection of mycotoxin. *Anal Chem* 92:8422–8426. <https://doi.org/10.1021/acs.analchem.0c01073>

25. Peltomaa R, Benito-Peña E, Moreno-Bondi MC (2018) Bioinspired recognition elements for mycotoxin sensors. *Anal Bioanal Chem* 410:747–771. <https://doi.org/10.1007/s00216-017-0701-3>

26. Chauhan R, Singh J, Sachdev T, Basu T, Malhotra BD (2016) Recent advances in mycotoxins detection. *Biosens Bioelectron* 81:532–545. <https://doi.org/10.1016/j.bios.2016.03.004>

27. Wild D (2013) The immunoassay handbook: theory and applications of ligand binding, ELISA and related techniques, 4th edn. Elsevier, Amsterdam

28. Zhao F, Wang H, Han X, Yang Z (2016) Development and comparative study of chemosynthesized antigen and mimotope-based immunoassays for class-specific analysis of *O,O*-dimethyl organophosphorus pesticides. *Sci Rep* 6. <https://doi.org/10.1038/srep37640>

29. Gazarian T, Selisko B, Héron P, Gazarian K (2000) Isolation and structure–functional characterization of phage display library-derived mimotopes of noxiustoxin, a neurotoxin of the scorpion *Centruroides noxius* Hoffmann. *Mol Immunol* 37:755–766. [https://doi.org/10.1016/S0161-5890\(00\)00091-2](https://doi.org/10.1016/S0161-5890(00)00091-2)

30. Liu J, Chisti MM, Zeng X (2017) General signal amplification strategy for nonfaradic impedimetric sensing: trastuzumab detection employing a peptide immunosensor. *Anal Chem* 89:4013–4020. <https://doi.org/10.1021/acs.analchem.6b04570>

31. Wang Y, Wang H, Li P, Zhang Q, Kim HJ, Gee SJ, Hammock BD (2013) Phage-displayed peptide that mimics aflatoxins and its application in immunoassay. *J Agric Food Chem* 61:2426–2433. <https://doi.org/10.1021/jf4004048>

32. He Z, He Q, Xu Y, Li YP, Liu X, Chen B, Lei D, Sun CH (2013) Ochratoxin a mimotope from second-generation peptide library and its application in immunoassay. *Anal Chem* 85:10304–10311. <https://doi.org/10.1021/ac402127t>

33. He Q, Xu Y, Zhang C, Li YP, Huang ZB (2014) Phage-borne peptidomimetics as immunochemical reagent in dot-immunoassay for mycotoxin zearalenone. *Food Control* 39:56–61. <https://doi.org/10.1016/j.foodcont.2013.10.019>

34. Barbas CFI, Burton DR, Scott JK, Silverman GJ (2001) Phage display: a laboratory manual. Cold Spring Harbor laboratory press. Cold Spring Harbor, NY, USA

35. Peltomaa R, López-Perolio I, Benito-Peña E, Barderas R, Moreno-Bondi MC (2016) Application of bacteriophages in sensor development. *Anal Bioanal Chem* 408:1805–1828. <https://doi.org/10.1007/s00216-015-9087-2>

36. Peltomaa R, Benito-Peña E, Barderas R, Moreno-Bondi MC (2019) Phage display in the quest for new selective recognition elements for biosensors. *ACS Omega* 4:11569–11580. <https://doi.org/10.1021/acsomega.9b01206>

37. Smartt AE, Ripp S (2011) Bacteriophage reporter technology for sensing and detecting microbial targets. *Anal Bioanal Chem* 400: 991–1007. <https://doi.org/10.1007/s00216-010-4561-3>

38. Peltomaa R, Benito-Peña E, Barderas R, Sauer U, González Andrade M, Moreno-Bondi MC (2017) Microarray-based immunoassay with synthetic mimotopes for the detection of fumonisin B<sub>1</sub>. *Anal Chem* 89:6216–6223. <https://doi.org/10.1021/acs.analchem.7b01178>

39. Zou X, Chen C, Huang X, Chen X, Wang L, Xiong Y (2016) Phage-free peptide ELISA for ochratoxin a detection based on biotinylated mimotope as a competing antigen. *Talanta* 146:394–400. <https://doi.org/10.1016/j.talanta.2015.08.049>

40. Liu R, Yu Z, He Q, Xu Y (2007) An immunoassay for ochratoxin a without the mycotoxin. *Food Control* 18:872–877. <https://doi.org/10.1016/j.foodcont.2006.05.002>

41. Peltomaa R, Agudo-Maestro I, Más V, Barderas R, Benito-Peña E, Moreno-Bondi MC (2019) Development and comparison of mimotope-based immunoassays for the analysis of fumonisin B1. *Anal Bioanal Chem* 411:6801–6811. <https://doi.org/10.1007/s00216-019-02068-7>

42. Peltomaa R, Amaro-Torres F, Carrasco S, Orellana G, Benito-Peña E, Moreno-Bondi MC (2018) Homogeneous quenching immunoassay for fumonisin B<sub>1</sub> based on gold nanoparticles and an epitope-mimicking yellow fluorescent protein. *ACS Nano* 12:11333–11342. <https://doi.org/10.1021/acsnano.8b06094>

43. Xu Y, Chen B, He Q, Qiu YL, Liu X, He ZY, Xiong ZP (2014) New approach for development of sensitive and environmentally friendly immunoassay for mycotoxin fumonisin B<sub>1</sub> based on using peptide–MBP fusion protein as substitute for coating antigen. *Anal Chem* 86:8433–8440. <https://doi.org/10.1021/ac502037w>

44. Xu Y, He Z, He Q, Qiu Y, Chen B, Chen J, Liu X (2014) Use of cloneable peptide–MBP fusion protein as a mimetic coating antigen in the standardized immunoassay for mycotoxin ochratoxin a. *J Agric Food Chem* 62:8830–8836. <https://doi.org/10.1021/jf5028922>

45. Ding Y, Hua X, Du M et al (2018) Recombinant, fluorescent, peptidomimetic tracer for immunodetection of imidacloprid. *Anal Chem* 90:13996–14002. <https://doi.org/10.1021/acs.analchem.8b03685>

46. Ding Y, Hua X, Chen H, Liu F, González-Sapien G, Wang M (2018) Recombinant peptidomimetic-nano luciferase tracers for sensitive single-step immunodetection of small molecules. *Anal Chem* 90:2230–2237. <https://doi.org/10.1021/acs.analchem.7b04601>

47. Tannous BA (2009) *Gaussia* luciferase reporter assay for monitoring biological processes in culture and in vivo. *Nat Protoc* 4:582–591

48. Moutsopoulos A, Hunt E, Broyles D, Pereira CA, Woodward K, Dikici E, Kaifer A, Daunert S, Deo SK (2017) Bioorthogonal protein conjugation: application to the development of a highly sensitive bioluminescent immunoassay for the detection of interferon-γ. *Bioconjug Chem* 28:1749–1757. <https://doi.org/10.1021/acs.bioconjchem.7b00220>

49. New England Biolabs (NEB) Ph.D. Phage Display Libraries - Instruction Manual. [www.neb.com/products/e8110-phd-12-phage-display-peptide-library-kit](http://www.neb.com/products/e8110-phd-12-phage-display-peptide-library-kit). Accessed 28 July 2020

50. Hunt EA, Moutsopoulos A, Ioannou S, Ahern K, Woodward K, Dikici E, Daunert S, Deo SK (2016) Truncated variants of *Gaussia* luciferase with tyrosine linker for site-specific bioconjugate applications. *Sci Rep* 6:26814. <https://doi.org/10.1038/srep26814>

51. Sulyok M, Berthiller F, Krska R, Schuhmacher R (2006) Development and validation of a liquid chromatography/tandem mass spectrometric method for the determination of 39 mycotoxins in wheat and maize. *Rapid Commun Mass Spectrom RCM* 20: 2649–2659. <https://doi.org/10.1002/rcm.2640>

52. Marco M-P, Gee S, Hammock BD (1995) Immunochemical techniques for environmental analysis I. Immunosensors. *Trends Anal Chem* 14:341–350. [https://doi.org/10.1016/0165-9936\(95\)97062-6](https://doi.org/10.1016/0165-9936(95)97062-6)

53. Zearalenone ELISA. Demeditec Diagn. GmbH. <https://www.demeditec.com/en/products/zearalenone-elisa-dezeae03>. Accessed 28 July 2020

54. Zearalenone ELISA Kit, Biovision. [www.biovision.com/zearalenone-zen-elisa-kit.html](http://www.biovision.com/zearalenone-zen-elisa-kit.html). Accessed 28 July 2020

55. AgraQuant® Zearalenone ELISA test, Romer Labs. [www.romerlabs.com/shop/romer\\_us\\_it/agraquant-r-zearalenone-elisa-test](http://www.romerlabs.com/shop/romer_us_it/agraquant-r-zearalenone-elisa-test). Accessed 28 July 2020

56. Chen Y, Zhang S, Hong Z, Lin Y, Dai H (2019) A mimotope peptide-based dual-signal readout competitive enzyme-linked immunoassay for non-toxic detection of zearalenone. *J Mater Chem B* 7:6972–6980. <https://doi.org/10.1039/C9TB01167F>

57. Fang D, Zhang S, Dai H, Li X, Hong Z, Lin Y (2019) Electrochemiluminescent competitive immunoassay for zearalenone based on the use of a mimotope peptide, Ru(II)(bpy)<sub>3</sub>-loaded NiFe<sub>2</sub>O<sub>4</sub> nanotubes and TiO<sub>2</sub> mesocrystals. *Microchim Acta* 186:608. <https://doi.org/10.1007/s00604-019-3714-0>

58. Maragos CM, Kim EK (2006) Cross-reactivity of six zearalenone antibodies in a hand-held fluorescence polarisation immunoassay.

In: Njapau H, Trujillo S, van Egmond H, Park D (eds) Mycotoxins and phycotoxins: advances in determination, toxicology and exposure management. Wageningen Academic Publishers

**Publisher's note** Springer Nature remains neutral with regard to jurisdictional claims in published maps and institutional affiliations.